# Comparison of Kernel Support Vector Machine Method Using Aerial Photographs to Identify Slum Settlements in Squatter Area of South Magelang

**Putri, T. A.,*  Hidayati, I. N.  and  Widayani, P.**
Department of Geographic Information Science, Universitas Gadjah Mada, Yogyakarta, Indonesia
E-mail: tifanny.ananda2103@mail.ugm.ac.id,*   iswari@ugm.ac.id,   primawidayani@ugm.ac.id
**Corresponding Author*

**DOI:  https://doi.org/10.52939/ijg.v22i7.5075**

**Abstract**
*Detection of slums in urban informal settlements plays an important role in making the right decisions and ensuring equitable urban growth in highly developing cities. This paper presents a comparative study of four types of SVM kernel functions, namely, Linear, RBF, Polynomial, and Sigmoid for classifying slum areas based on texture feature using Gray Level Co-occurrence Matrix (GLCM) from very high resolution aerial images. The study is performed with a sample squatter area in South Magelang, Magelang City, Indonesia, and compares the performance of three essential GLCM features (mean, variance, and dissimilarity) on different window sizes. As can be seen, there is a considerable impact of kernel type selection in classification performance. The best performance in terms of overall accuracy was obtained by using RBF kernel with a relatively low accuracy of 62.26%, then comes Polynomial (57.78%), Linear (55.33%), and Sigmoid (49.72%). The above hierarchy of performance shows the fundamental non-linearity that exists between the morphology of slums and the textural representation of slums in the RGB image. Majority voting aggregation of the output of texture feature extraction for each kernel resulted in more coherent settlement maps. In summary, this study offers empirical evidence to guide the optimal use of SVM-based texture features in slum mapping, providing a screening procedure for the automated analysis of urban morphologies via remote sensing.*

**Keywords:** Aerial Image, Geospatial Machine Learning, Support Vector Machine (SVM), Texture Feature Extraction, Urban Slum Identification

## 1. Introduction

The increasing speed of urbanization in developing nations is causing the occurrence of informal settlements known as slums that constitute a serious problem for sustainable urban planning, public health, and social justice [1]. In the case of Indonesia, cities like Magelang city suffer from constant problems regarding the expansion of slums, mainly due to the high levels of rural-urban migration and competition for urban land uses [2]. For proper urban planning and implementation of structural solutions like the *Kota Tanpa Kumuh* (KOTAKU) project, precise spatiotemporal information about the properties of informal settlements is essential [3]. Traditional approaches based on field surveying and visual interpretation are highly resource and labor intensive and non-scalable for periodical monitoring [4]. Hence, remote sensing by use of Very High Resolution (VHR) datasets has become an indispensable tool in carrying out objective synoptic analyses of the urban environment, allowing the detection of morphological features such as high building density, irregular layout, and heterogeneity of the built-up area [5]. Though VHR aerial images provide remarkable spatial resolution, freely available and affordable datasets are normally limited to RGB spectral bands only, hampering the performance of traditional spectral classifiers [6]. Therefore, in order to overcome the problem of limited spectral resolution, texture extraction has been widely applied to describe the arrangement of tones in the image. One of such approaches is the use of the Gray Level Co-occurrence Matrix (GLCM) in order to characterize urban fabric using its second order features (mean, variance, and dissimilarity) that capture density, heterogeneity of structure size, and irregularity of layout[7].

Recently, however, the area of informal settlement mapping is leaning more towards the use of SOTA deep learning models such as CNN and semantic segmentation methods [8] and [9]. However, while these methods exhibit good performance in macroscopic urban classification tasks, they are data hungry, computationally costly, and depend too much on large amounts of quality labeled data that are often lacking in regional municipal planning scenarios [10]. As a result, more sophisticated classifiers from the realm of classical machine learning, such as the Support Vector Machine (SVM), have not lost their importance. In particular, SVM proved to be superior in dealing with high-dimensional feature spaces and finding an optimal non-linear separating line despite relatively small training sample size, which makes it a good option for local urban zoning [11].

SVM's performance depended intrinsically on the type of kernel that implicitly projects the input into higher-dimensional space for class separation. Though various kernels such as linear, polynomial, radial basis function (RBF), and sigmoid enable different capabilities of modeling complicated geometry in data, an empirical assessment of the performance of all these kernels in GLCM-based slum detection has not been extensively conducted yet. Earlier works on the subject have been mostly limited to one specific kernel or the general SVM algorithm versus other machine learning techniques without considering kernel performance alone [12]. Moreover, the scale of analysis, defined through the GLCM window size, greatly impacts feature extraction from textures. Small windows allow localized information but with high probability of noise, whereas large windows help in identifying larger context patterns but flatten the structural edges [13]. The scale-dependency needs a systematic analysis specific to the local urban morphology in order to determine the right combination of kernel functions and scales.

The objective of this study was to conduct systematic comparisons of four kernel functions of the SVM approach (linear, radial basis function, polynomial, and sigmoid) to classify slum zones based on multi-scale GLCM texture characteristics obtained from ultra-high resolution aerial imagery. In particular, the research goals were to: (1) examine the ability of the use of different GLCM characteristics and window size to describe the morphological aspects of slums; (2) examine the effect of kernel function on the accuracy of classification; and (3) generate a high-quality slum area map for specific kelurahan in South Magelang District to support localized urban upgrading strategies.

## 2. Material and Method

### *2.1 Study Area*

The study was carried out in the city of Magelang which is situated at coordinates of longitude 110°12′30″ to 110°12′52″ East and latitude 7°26′18″ to 7°30′9″ South at about 337 meters above sea level. The study area was presented in Figure 1. The current research involved the analysis of part of the South Magelang District. The South Magelang District was chosen as the location for conducting the study since it encompasses the biggest spatial coverage of slum-related areas within the city. The size of the South Magelang District is approximately 713 hectares which is larger than that of Central and North Magelang districts. The areas of districts are presented in Table 1. Regarding the distribution of the slums, the South Magelang District shares a considerable share of the entire slum coverage of the city at 53.10%, followed by the Central Magelang District and the North Magelang District, sharing 2.80% and 44.10%, respectively, according to data obtained from the Housing and Settlement Area Office of Magelang City. Furthermore, the study site also consists of the former railway lands owned by PT Kereta Api Indonesia (PT KAI), which have been illegally occupied throughout the years. This area was characterized with the settlement of squatters along railway routes. Such an illegal settlement area forms a complex pattern and becomes an important consideration in analyzing the slum classification through remote sensing and machine learning methods.

### *2.2 Data Collection*

The data used in this research were remotely sensed image and accompanying geospatial data to aid in the accurate identification and analysis of the characteristics of slum settlement areas. The main data were a 2023 aerial image in raster format from the Department of Public Works and Spatial Planning (DPUPR). This data has very high spatial resolution that can be used to identify the morphology of the urban area. Other spatial data in vector format are administrative boundary, road network, and river data from TanahAir Indonesia (tanahair.indonesia.go.id) which were used as base map data. Furthermore, ground truth data in vector format were also collected in field survey and consist of validated data of slum and non-slum settlements. Field survey data were crucial in the process of training and testing the classification model, ensuring that the analysis reflects actual on-site conditions. The specifications of the data used in the study are presented in Table 2.

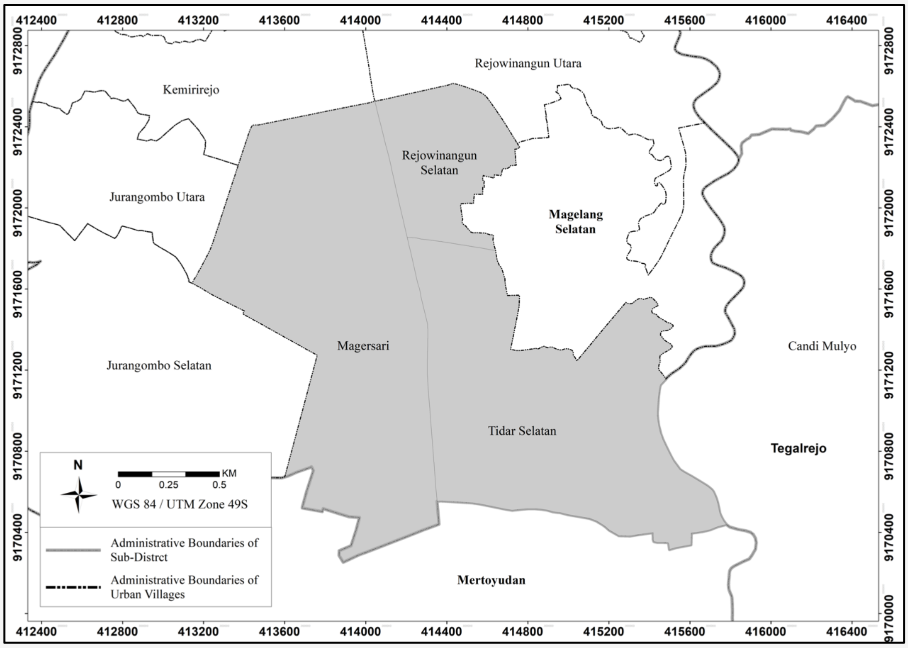


**Figure 1:** Study Area of part of South Magelang District and surrounding districts

**Table 1:** Area extent in Magelang city by district

| No. | City | District | Total Area (ha) |
|---|---|---|---|
| 1 | | South Magelang | 713 |
| 2 | Magelang | Central Magelang | 510 |
| 3 | | North Magelang | 631 |

**Table 2:** Specifications of the data used in the research

| No. | Data | Type | Source |
|---|---|---|---|
| 1 | Aerial Photograph (2023) | Raster | Department of Public Works and Spatial Planning (DPUPR) |
| 2 | Administrative Boundaries, Road, and River | Vector | tanahair.indonesia.go.id |
| 3 | Ground Truth | Vector | Field Survey Results |

*2.3 Methodology*

*2.3.1 Data preparation and sample generation*

In the first step, the preparation of the ultra-high-resolution (GSD = 4.9 cm) RGB aerial mosaic image of Magelang city was done. In order to increase computational efficiency but not sacrifice the important structural information, the images were down-sampled to GSD = 25 cm by cubic convolution resampling method [14]. The reason for selecting this technique was that it would maintain the edge sharpness and reduce spectral distortion. The training and validation data sets were created through a stratified random sampling method inside the ground-truthed slum and non-slum polygons. In order to achieve statistical efficiency, the minimum number of samples needed were calculated through Slovin's formula with 5% error margin as presented in Equation 1 [15]:

$$n = \frac{N}{1 + Ne^2}$$

Equation 1

With $N$ being the number of all the pixels in the residential area and $e$ = 0.05. From this equation, a balanced dataset having 9,000 pixels was developed by assigning 4,500 pixels each to the two categories of slum and non-slums. Minimum distance between the sampling points was also ensured to avoid spatial auto-correlation [16]. The last data set was split according to polygon boundaries where 70% of the data set (6,300 pixels) formed the training set while 30% of the data set (2,700 pixels) formed the testing set.

*2.3.2 Residential building object extraction*

To narrow down the classification process to only the residential built-up areas while reducing the noise caused by other irrelevant attributes like trees, shadows, water bodies, and large asphalt roads, a masking process in space was introduced [17]. The aerial images were cropped using a Geographic Information System environment using the vector data representing the building footprints derived from the same aerial image and checked during ground surveys [18]. Pixels lying outside the pre-defined residential areas were masked with null values, while those lying inside were retained. Object-oriented masking process enables an increase in signal-to-noise ratio in the feature space, hence enabling the texture algorithms to concentrate solely on the changes in roof and building textures and spatial layouts.

*2.3.3 Multi-scale texture feature extraction*

The texture variations were calculated using the method known as the Gray Level Co-occurrence Matrix (GLCM) [19]. For a spatial displacement vector (*Δx*, and *Δy*), the GLCM $P_{d,\theta}$ was a square matrix of dimension $N_g \times N_g$ (where $N_g$ is the number of gray levels), while $P(i,j)$ is the probability of transitioning from gray level $i$ to gray level $j$ as presented in Equation 2:

$$p(i,j) = \frac{((x_1,y_1),(x_2,y_2)) \in R \times R \mid f(x_1,y_1) = i, f(x_2,y_2) = j}{R}$$

Equation 2

Where $R$ is the selected image window and $f(x,y)$ epresents pixel intensity values. Three features of the second-order statistics were used owing to the known ability of discrimination of the informal urban texture as presented in Equation 3, Equation 4, and Equation 5 [20]:

$$Mean\ (\mu) = \sum_{i=0}^{N_g-1} \sum_{j=0}^{N_g-1} i \cdot p(i,j)$$

Equation 3

$$Variance\ (\sigma^2) = \sum_{i=0}^{N_g-1} \sum_{j=0}^{N_g-1} p(i,j)(i-\mu)^2$$

Equation 4

$$Dissimilarity\ (D) = \sum_{i=0}^{N_g-1} \sum_{j=0}^{N_g-1} p(i,j) \mid i-j \mid^2$$

Equation 5

In order to take care of the scale dependency of urban morphology, the window size selection was initially based on the actual physical dimension of the roof of the residential buildings within the study area. It is based on visual interpretation that the average physical dimension of the roof is around 9 meters, which equals 36 pixels using the re-sampled resolution of 25 cm. The physical dimension of the roofs is considered to establish the upper boundary scale in the GLCM analysis framework. A 37×37 pixel window will therefore be considered, taking into account that it should be odd due to the moving window nature of the GLCM analysis which involves a central pixel for symmetric spatial analysis.

As a means of dealing with the scale dependency problem, these features were extracted using three window sizes in square form namely 9x9, 19x19, and 37x37 pixels. In relation to the resampled 25 cm GSD data, these specific scales translate to ground dimensions of about 2.25 meters, 4.75 meters, and 9.25 meters respectively. The 9x9 window size is for micro-texture (single roofing material variation), while the 19x19 window size is the size of small buildings, and 37x37 window size refers to macrocontextual arrangements (neighborhoods blocks and building to void configurations). All the metrics were calculated at four orientations (0°, 45°, 90°, 135°) and averaged to maintain direction invariance.

*2.3.4 Feature stacking and dataset creation*

After the process of multi-scale texture extraction, there is an important process of data integration, which combines the heterogeneous variables together. The 27 extracted texture layers in total, three GLCM features computed at three different scales for each of the three spectral bands, were mathematically integrated with the three original RGB spectral bands through layer stacking to form a new 30-dimensional composite raster dataset [21] as presented in Figure 2. Such process is quite necessary to reflect the multiple aspects of complicated urban morphology, but the original RGB bands can only reflect the material reflectance, the stacked multi-scale GLCM layers represent the spatial arrangement and structural heterogeneity of such urban materials. In the course of this process, the consistency in coordinate system, same spatial resolution, and the same spatial extent were strictly kept among all raster layers to avoid the pixel shift problem that may impair the capability of model learning.

With the definition of the multidimensional feature space in place, sampling was done on the geographic space to facilitate transformation of the data from the geospatial raster form to the statistical tabular form. Pixel values for all the 30 bands were extracted accurately at the geographic location of the predetermined sample points. In order to maintain the statistical quality of the original feature values, this process of point-by-point extraction was carried out without any further resampling or interpolation artifact being used. The multidimensional arrays that were obtained after extraction were structured in the form of a Comma Separated Values (CSV) matrix. In this database, each row consisted of one pixel observation while the columns included the corresponding spectral and textural predictor variables. Additionally, each observation was labeled with important metadata information such as point identifier, polygon ID, and most importantly the ground-truth classification labels (*slum/non-slum*). This systematic structuring of the data facilitated the linking of the spatial GIS domain to the statistical machine learning domain and made the high dimensional data set ready for the subsequent SVM learning and validation pipelines [22].

*2.3.5 Support vector machine classification and tuning*

Classification phase used the support vector machine (SVM) classifier, a supervised machine learning algorithm known for its effectiveness in dealing with high dimensional and complex data in remote sensing [11]. SVM was especially suitable for this research as the multi-scale and spectral features create a multidimensional feature space where it becomes difficult for normal classifiers to achieve optimal decision boundaries as shown in Figure 3. The following kernel functions were tested to find out the optimal decision boundary that separates slum from non-slum neighborhoods: Linear Kernel, Polynomial Kernel, Radial Basis Function Kernel, and Sigmoid Kernel as shown in Figure 4. The function was used to transform input data into the required feature space in order to make linear and non-linear separation possible.

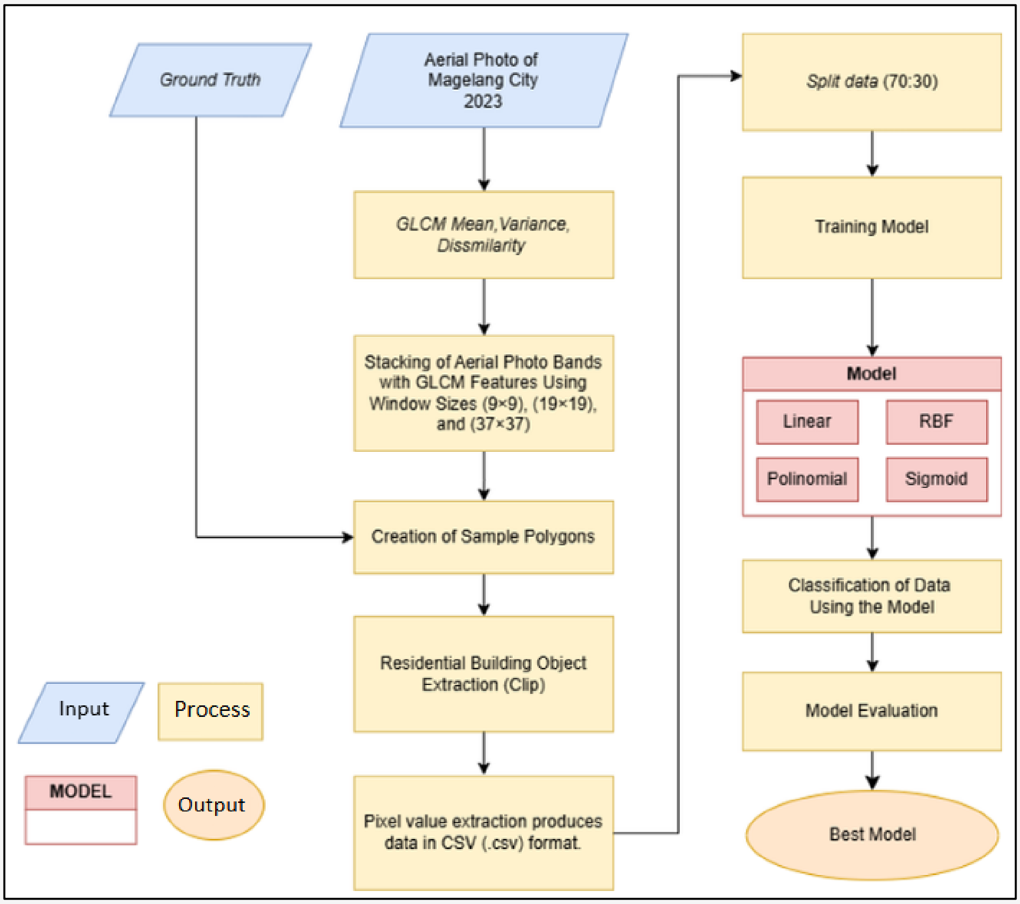


**Figure 2:** Methodological flowchart of the proposed SVM-GLCM framework


ISSN: 1686-6576 (Printed) | ISSN 2673-0014 (Online) | © Geoinformatics International

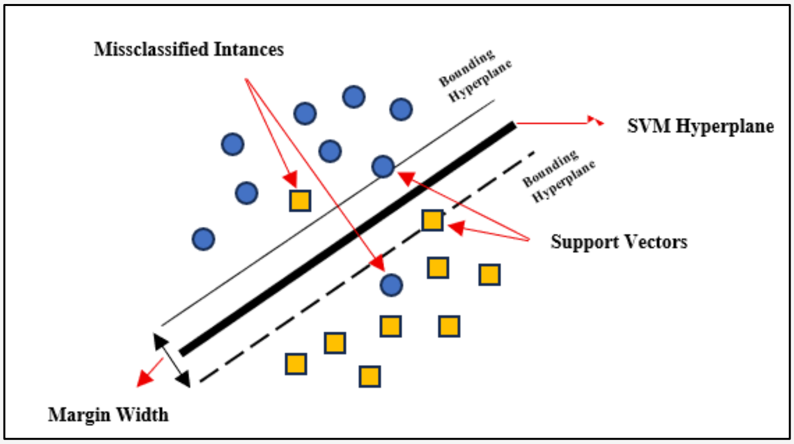


**Figure 3:** Support vector machine

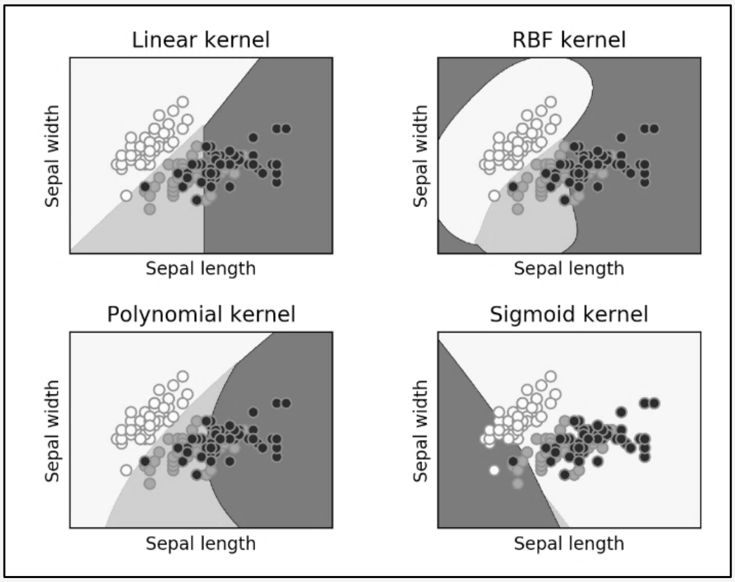


**Figure 4:** Kernel support vector machine

As explained in the sample generation process, the dataset was split in such a way that 70% is used for training data and 30% for independent testing data, which is the most frequently used ratio balancing both aspects of learning and evaluation [23]. Optimal performance in SVM largely depended on tuning of hyperparameters; consequently, grid search along with five-fold cross validation was used on the training data set [24]. In case of the linear kernel, the parameter C that helps to tune the margin of maximum and misclassification tolerance needs to be optimized. The Polynomial kernel requires the optimization of degree of polynomial and *C*. In case of RBF kernel, *C* and gamma ($\gamma$), need to be optimized, while the same is the case with sigmoid kernel. Such validation technique reduced overfitting by checking the stability of models on different training sets. Once optimized, the models were then deployed on the test dataset. The performance of these models was analyzed based on well-known accuracy measures, such as OA (overall accuracy), precision, recall, F1 score, and kappa coefficient [25]. Considering the operational importance of slum identification, great attention was paid to the recall and precision of the slum class in order to reduce omission and commission errors [5]. In conclusion, this comparative approach facilitated the selection of the best possible kernel function to be used in modeling the settlement morphology, thus allowing a practical foundation for the non-linear texture classification in urban remote sensing.

## 3. Result and Discussion

### *3.1 Influence of GLCM Window Size and Feature Importance*

A comparative analysis of the texture features was done in order to find out the relation between the features and classification accuracy by using the


ISSN: 1686-6576 (Printed) | ISSN 2673-0014 (Online) | © Geoinformatics International

class-wise mean values and visualizations. From the analysis, it was found that the Dissimilarity and Mean features with the window size of 9×9 performed very strongly in differentiating between slum and non-slum categories as their mean values had the highest difference between these two categories. Besides, Variance with window size 37×37 also produced good class separation. Overall, the higher the difference in mean values between the classes, the higher would be the discriminatory capacity of the features.

The comparative analysis of the texture features obtained using the GLCM method, i.e., mean, variance, and dissimilarity was presented in Figure 5. Below the graphs showed class-wise average values for the slum and non-slum regions on different spectral bands (Red, Green, and Blue) for different window sizes (9x9, 19x19, and 37x37 pixels). Through the line plots, the variations in the behavior of the features for the two classes could be observed which helps in understanding the difference between them. This also made it easy to understand how the feature behaves with the change in scale and the efficiency of the feature in segregating the informal settlement from the formal one. From the output of visualizations at Figure 6, a noticeable trend is evident in all the features and especially in those that are smaller in window size. The 9×9pixel window (~2.25 m ground dimension) appeared to provide the highest separability between classes, which implies that textural differences at a very small scale have a significant influence on the classification of slums versus non-slums. At this scale, the textural information from small urban objects is retained without much smoothing, allowing fine-grained spatial patterns to remain distinguishable.

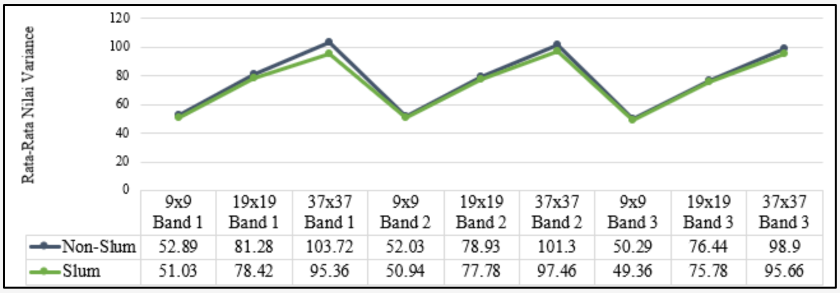


| | 9x9 Band 1 | 19x19 Band 1 | 37x37 Band 1 | 9x9 Band 2 | 19x19 Band 2 | 37x37 Band 2 | 9x9 Band 3 | 19x19 Band 3 | 37x37 Band 3 |
|---|---|---|---|---|---|---|---|---|---|
| Non-Slum | 52.89 | 81.28 | 103.72 | 52.03 | 78.93 | 101.3 | 50.29 | 76.44 | 98.9 |
| Slum | 51.03 | 78.42 | 95.36 | 50.94 | 77.78 | 97.46 | 49.36 | 75.78 | 95.66 |

(a)

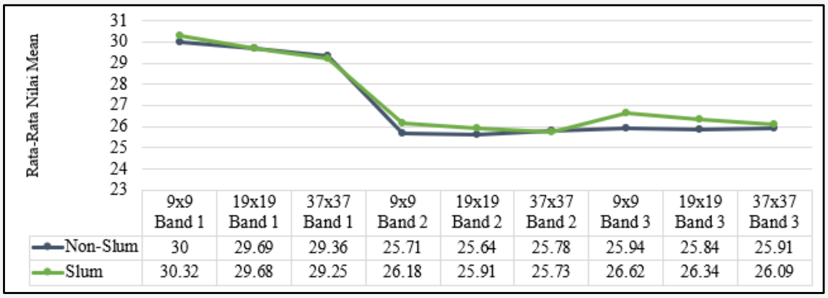


| | 9x9 Band 1 | 19x19 Band 1 | 37x37 Band 1 | 9x9 Band 2 | 19x19 Band 2 | 37x37 Band 2 | 9x9 Band 3 | 19x19 Band 3 | 37x37 Band 3 |
|---|---|---|---|---|---|---|---|---|---|
| Non-Slum | 30 | 29.69 | 29.36 | 25.71 | 25.64 | 25.78 | 25.94 | 25.84 | 25.91 |
| Slum | 30.32 | 29.68 | 29.25 | 26.18 | 25.91 | 25.73 | 26.62 | 26.34 | 26.09 |

(b)

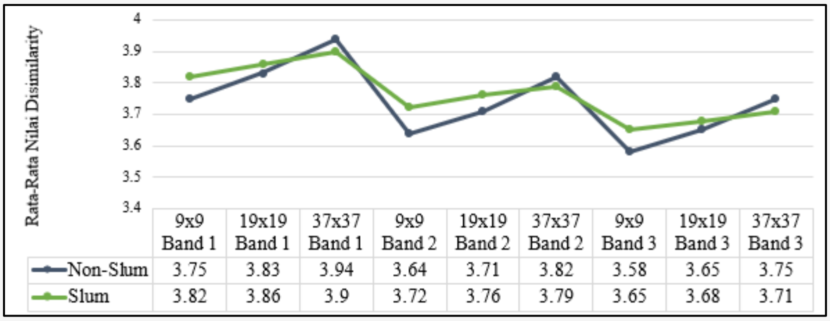


| | 9x9 Band 1 | 19x19 Band 1 | 37x37 Band 1 | 9x9 Band 2 | 19x19 Band 2 | 37x37 Band 2 | 9x9 Band 3 | 19x19 Band 3 | 37x37 Band 3 |
|---|---|---|---|---|---|---|---|---|---|
| Non-Slum | 3.75 | 3.83 | 3.94 | 3.64 | 3.71 | 3.82 | 3.58 | 3.65 | 3.75 |
| Slum | 3.82 | 3.86 | 3.9 | 3.72 | 3.76 | 3.79 | 3.65 | 3.68 | 3.71 |

(c)

**Figure 5:** Comparison of feature average values: (a) Variance (b) Mean (c) Dissimilarity


ISSN: 1686-6576 (Printed) | ISSN 2673-0014 (Online) | © Geoinformatics International

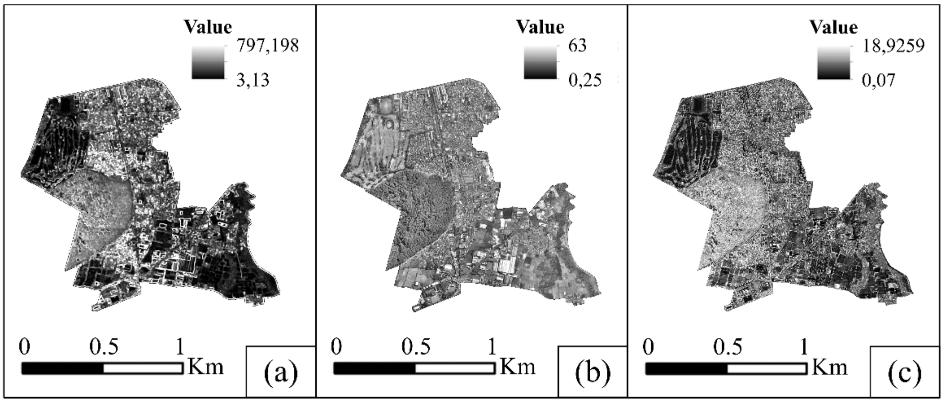

**Figure 6:** Comparative analysis of texture features: (a) Variance (b) Mean (c) Dissimilarity

**Table 3:** Performance metrics of the optimized SVM classifiers

| Kernel | Optimal Parameters | Overall Accuracy (%) | Precision (Slum) | Recall (Slum) | F1-Score (Macro Avg.) |
|---|---|---|---|---|---|
| **RBF** | C = 100<br>gamma = 'auto' | 62.26 | 0.61 | 0.67 | 0.62 |
| **Polynomial** | C = 100<br>degree = 3<br>gamma = 'scale'<br>coef0 = 1 | 57.78 | 0.57 | 0.62 | 0.58 |
| **Linear** | C = 0.01 | 55.33 | 0.55 | 0.64 | 0.55 |
| **Sigmoid** | C = 0.1<br>gamma = 'auto',<br>coef0 = 0 | 49.72 | 0.50 | 0.52 | 0.50 |

Apart from Dissimilarity, the feature named "Mean" derived using the 9 × 9 window size also possessed good discriminative capacity. Mean was the mean value of gray-level intensities of the pixels in a neighborhood and indicated the general tonal properties of the observed surface. As a result of heterogeneity of the roofs and buildings in slums, as well as high building density, different tonal properties arise. So, Mean and Dissimilarity features provide complementary information, with the latter stressing the spatial irregularities [26]. With the increasing size of the windows, multi-scale analysis showed a slow loss of local details because of the averaging effect. With the window size of 19×19 (~4.75 m), the neighborhoods could be represented, although the fine structural transition between roof components and narrow gaps is beginning to be smoothed. On the other hand, with the 37×37 (~9.25 m) window size, more global context can be captured where spatial heterogeneity is more visible at the block scale.

At this larger scale, Variance demonstrates relatively strong discriminatory performance by capturing the degree of intensity dispersion within a settlement block. Higher variance values indicate greater heterogeneity in surface composition, including variations in building structure, open spaces, vegetation, and road networks. However, the increased spatial extent also reduced sensitivity to localized irregularities, which are key characteristics of slum boundaries and fragmented settlement patterns [27]. In general, the use of multi-scale texture features offers a more complete description of urban morphology. The use of micro-scale texture features, which include Mean and Dissimilarity at scale 9×9, together with macro-scale heterogeneity, that is, Variance at scale 37×37, improves the separability of slum and non-slum areas. This improves the performance of classification.

*3.2 Comparative Analysis of SVM Kernels*

Results obtained from the performance evaluation of the four SVM kernels using the independent test set (n=2,700) revealed that RBF kernel performed best in terms of overall accuracy (OA: 62.26%) and macro-averaged F1-score (F1: 0.62) as shown in Table 3. It was followed by Polynomial kernel (OA: 57.78%, F1: 0.58), Linear kernel (OA: 55.33%, F1: 0.55), and finally, the Sigmoid kernel (OA: 49.72%, F1: 0.50). The above-mentioned performance trend revealed different levels of ability to model complex and non-linear decision boundary necessary for separation of slum and non-slum pixels with regard to their spectral textural signatures extracted using


ISSN: 1686-6576 (Printed) | ISSN 2673-0014 (Online) 

GLCM texture features [28]. Overall, from the results obtained, we stated that the better is the ability to model non-linear decision boundaries, the higher is the classification performance since this feature is very important in the urban environment where slum and non-slum areas may have similar visual/textural characteristics.

The grid search method for hyperparameter optimization yielded different optimal settings for each kernel since each kernel is sensitive to its parameters differently in the same feature space. In this case, the RBF kernel had a high regularization parameter value (C=100) and gamma = 'auto' which made it possible to detect the fine texture variation like contrast and spatial heterogeneity and discontinuities of urban fabric [29]. For ensuring that the tuning procedure of the model is robust, the grid search covered an extensive range of parameters including C parameter values from $10^{-2}$ to $10^{3}$ and $\gamma$ parameter values from$10^{-3}$ to $10^{1}$. In addition, the optimal setting for RBF kernel ($C = 100, \gamma =$ 'auto') lied in the inner part of the parameter search space rather than the border. It means that the solution has found a robust region where the models perform effectively without being a result of the parameter borders.

The outstanding performance of the RBF kernel from the methodology point of view was explained with the help of its ability to map input features to a high-dimensional space using Gaussian similarity function. This helped the model to draw adaptive decision boundaries, which are crucial for the distinction of slum and non-slum classes with high variability and overlapping. In dense urban environments, the slum formation was described through irregular building layouts, heterogeneous roofing, different building sizes, and fragmented distribution. All of this leads to complicated distributions of textures that cannot be separated with the help of linear decision boundaries.

On the other hand, the Linear kernel performed optimally at low values of C (0.01), implying that it favored a large margin with high misclassification tolerance. Although this parameter works well in cases where the data is linearly separable, it is quite limited in our scenario because of the inherently non-linear nature of the features extracted from GLCM. Features like mean, variance, and dissimilarity consider spatial variations at both micro and macro levels hence the heterogeneity of the feature space is quite pronounced and non-linearly separable [4] and [30]. In this case, the Linear kernel is limited in terms of its ability to generate the required decision boundary by a hyperplane only. This made it inadequate for capturing the complexity of urban texture and poor performance results.

In comparison with the Linear kernel, the Polynomial kernel ($d = 3$) showed better flexibility due to non-linear interaction of features via polynomial transformation. Nevertheless, its efficiency is still inferior to that of the RBF kernel. The main reason for that is the global nature of the polynomial transformation in the feature space. Changes made in one place affect another part of the model. In heterogeneous urban settings, this usually results in over-generalization, when small local discontinuities of texture are ignored. That is why the Polynomial kernel tends to classify medium density formal settlements as slums, which means that it loses sensitivity to local discontinuities. Despite parameter optimization, the models with the Polynomial kernel remain rigid due to their natural structure of transformation. Thus, they cannot adapt to very heterogeneous urban textures [12].

Sigmoid kernel yielded the worst performance (OA: 49.72%) because it used hyperbolic tangent, which is not compatible with texture classification in the dataset. It is worth noting that the sigmoid kernel has similar behavior to the neural network activation function but it is highly sensitive to the stability of parameters and distribution of data. As a result of high dimensional remote sensing datasets generated by GLCM features, feature space may have overlapped class distribution and may not be Gaussian distributed, thus causing unstable decision boundaries with the use of the Sigmoid kernel [11] and [30]. Such a situation leads to an unstable distribution between the slum and non-slum class, hence is the least efficient kerntel for the set of kernels under study. While the Sigmoid kernel is capable of handling non-linear mappings in theory, the dependency of the results on the parameters C, gamma, and coef0 makes the algorithm less robust than the other two kernels. This problem is more evident when applied to heterogeneous cities, where there is more feature intersection and low class separability.

In general, the obtained results showed that the choice of kernel had great significance in defining the performance of classification in texture-based urban mapping. The RBF kernel always achieved better results than the other kernels because of its ability to model localized non-linear patterns in feature spaces. However, although being the most accurate model, the accuracy rate of 62.26% indicated an average result for binary classification. This showed that although GLCM texture descriptors contain some discriminatory information, they are not enough to completely capture the complexity of urban structure in slum and non-slum areas. Improving these models could be done using other spectral or structural features or even multi-sensor data. Since the RBF


ISSN: 1686-6576 (Printed) | ISSN 2673-0014 (Online) | © Geoinformatics International

kernel had shown the best performance of all the investigated kernels, obtaining 62.26% of accuracy and 0.62 of macro-averaged F1-score, additional investigations were performed in order to evaluate the behavior of this kernel along with its parameter robustness. First, the classification performance of the chosen model was evaluated via a confusion matrix as shown in Table 4. It presented the detailed information on true positives, true negatives, false positives, and false negatives. Second, the heatmap of grid search results was produced to estimate the stability of the chosen parameters over the search space. The heatmap was presented in Figure 7.

According to the confusion matrix, the TP value is 88,396, TN value is 2,370,962, FP value is 2,233,740, and FN value is 95,378. It can be observed from these values that while the model has the ability to classify the vast majority of non-slum pixels, it is producing a fairly large number of classification errors mainly due to the False Positive type. In other words, the confusion matrix reveals that there is still a considerable similarity between the slum and non-slum classes. It means that the model has difficulties distinguishing these classes from each other. Therefore, overall, the confusion matrix shows that the model has quite decent classification capabilities, although it could be made better to reach higher accuracy and precision. To further assess the consistency of the model performance in terms of various hyperparameters settings, an additional analysis of the grid search results was done using a heatmap visualization approach. The heatmap was built by analyzing the results of a thorough grid search with cross-validation. Here, the dataset was split into training and validation parts using k-fold cross-validation several times to make sure that the performance estimation is independent of the particular data split. In addition, for each k-fold split, the RBF kernel SVM was trained using various sets of parameters, and its performance was measured with the macro-averaged F1 score. This approach provided a set of performance metrics reflecting the model generalization on various subsets of the dataset.

The scores of all acquired performances were later put in order by arranging them into a matrix, with cells that are representative of individual combinations of parameters used for testing during the grid search procedure. The matrix thus gives an overall view of the model's behavior throughout the entire search space. The values contained in the matrix were later transformed into a two-dimensional heatmap form, whereby color intensity is proportional to classification performance. Darker colors represent high F1-scores, while lighter colors show low performance regions. In this study, it can be seen from the heatmap that there is an apparent distribution of performance in which high-performing regions are clearly marked and are consistently distributed and not just randomly occurring peaks.

**Table 4:** Confusion matrix

| **Actual Class** | **Predicted Slum** | **Predicted Non-Slum** |
|---|---|---|
| Slum | 88,396 (True Positive, TP) | 95,378 (False Negative, FN) |
| Non-Slum | 2,233,740 (False Positive, FP) | 2,370,962 (True Negative, TN) |

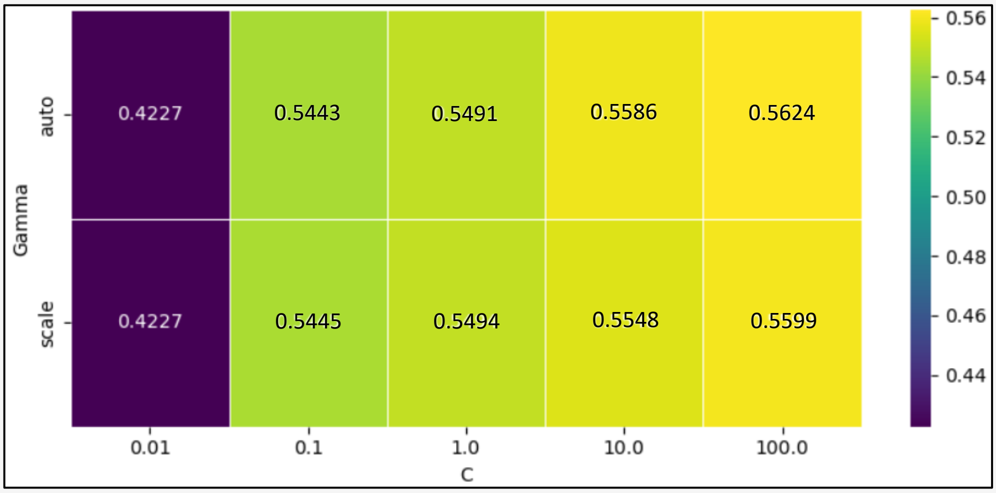


**Figure 7:** Heatmap of grid search results for RBF SVM hyperparameter tuning


ISSN: 1686-6576 (Printed) | ISSN 2673-0014 (Online) | © Geoinformatics International

This means that the chosen RBF kernel setting was not only the best choice numerically but also gives stable performance in terms of behavior. Therefore, the heatmap supports the conclusion that the RBF kernel gives good and stable performance in classifying slums and non-slums using GLCM textures.

The results indicate that performance becomes better when C takes larger values, where the best results are achieved at C = 100. It can be concluded that models with less regularization ability better learn complicated data structures, while a small value of C results in underfitting. As for gamma, its impact on performance was not very noticeable; however, it should be mentioned that gamma 'auto' worked better in case of large values of C. On average, the impact of C is stronger than that of gamma. Thus, one can conclude that model performance is more affected by the level of regularization than by the properties of kernel scaling. Heatmaps prove that the optimal parameters (C = 100, gamma = 'auto') are located in a stable high-performing area, which allows considering RBF models' results as reliable.

### *3.3 Visual Analysis of GLCM Texture Classification Results*

Visual interpretation of the obtained classification maps shown in Figure 8 demonstrated visible distinctions in spatial distribution of slums and non-slum settlements between the different SVM kernels under consideration. In general, these distinctions are similar to the results achieved by the quantitative evaluation measures and provide further information about the capability of the kernels to differentiate between settlements using GLCM texture features. Among the three GLCM features, the Mean feature generally produced smoother classification patterns, whereas the Variance and Dissimilarity features highlighted local texture heterogeneity more effectively, resulting in clearer delineation of slum and non-slum settlement boundaries.

The obtained classification map for the case of the Linear kernel showed a rather generalized spatial pattern. Classified areas in the slum settlements usually occur in big uniform clusters and not sensitive to local texture variations. While it is able to classify the big dense settlement areas, there seems to be a problem in classifying the transition areas of slums from non-slums. The cause of this can be linked to the linear decision boundary that fails to capture the non-linear relationship of texture features. This limitation was more apparent when using the Mean feature, while the additional texture information provided by the Variance and Dissimilarity features only slightly improved the representation of heterogeneous settlement areas. As such, some urban heterogeneity zones are categorized too simplistically, which causes loss in spatial information and leads to inaccurate depiction of settlement morphology.

The Polynomial Kernel Classification indicated that there is an improvement in the detection of local variations in texture. The classification map has identified more slum settlement clusters and provides more details for delineating boundaries of settlements. This improvement was more noticeable for the Variance and Dissimilarity features, which visually captured local texture variation more effectively than the Mean feature. Nevertheless, there are some scattered and isolated pixels detected in the classified image, especially in the zones having medium-density housing. This fragmentation indicated that the Polynomial Kernel was flexible enough to model the relationships between features but could lead to local classification errors where classes have similar texture properties. Consequently, certain sections of formally organized residential neighborhoods were categorized as slums, making it impossible to achieve uniformity in the mapping process. The resulting classification map from the Radial Basis Function (RBF) kernel showed the highest spatial consistency for all tested kernels. There are defined clusters corresponding to visually dense irregular settlements in areas with slum settlements. The resulting clusters of pixels contain less noise in comparison with results obtained using the Linear and Polynomial kernels. In addition, there are less fragmented groups of classified pixels. Thus, the usage of the RBF kernel allows building better models in terms of modeling of the complex nonlinear relations in the multi-dimensional space of GLCM features. The improvement was especially evident for the Variance and Dissimilarity features, which produced more compact slum clusters and clearer separation from non-slum settlements. Similar textures are combined into clusters more consistently which leads to clearer differentiation between slum and non-slum settlements. The decrease of salt-and-pepper effect in the resulting clusters proves the ability of the RBF kernel to model localized texture features and spatial consistency.

On the other hand, Sigmoid kernel classification represented the least stable spatial pattern. The pixels associated with slums seem to be highly fragmented, and there are no clear clusters formed throughout the test site. There are also several isolated pixels seen in both slums and non-slums, implying that it is difficult to form a stable decision boundary from the texture features derived.


ISSN: 1686-6576 (Printed) | ISSN 2673-0014 (Online) | 

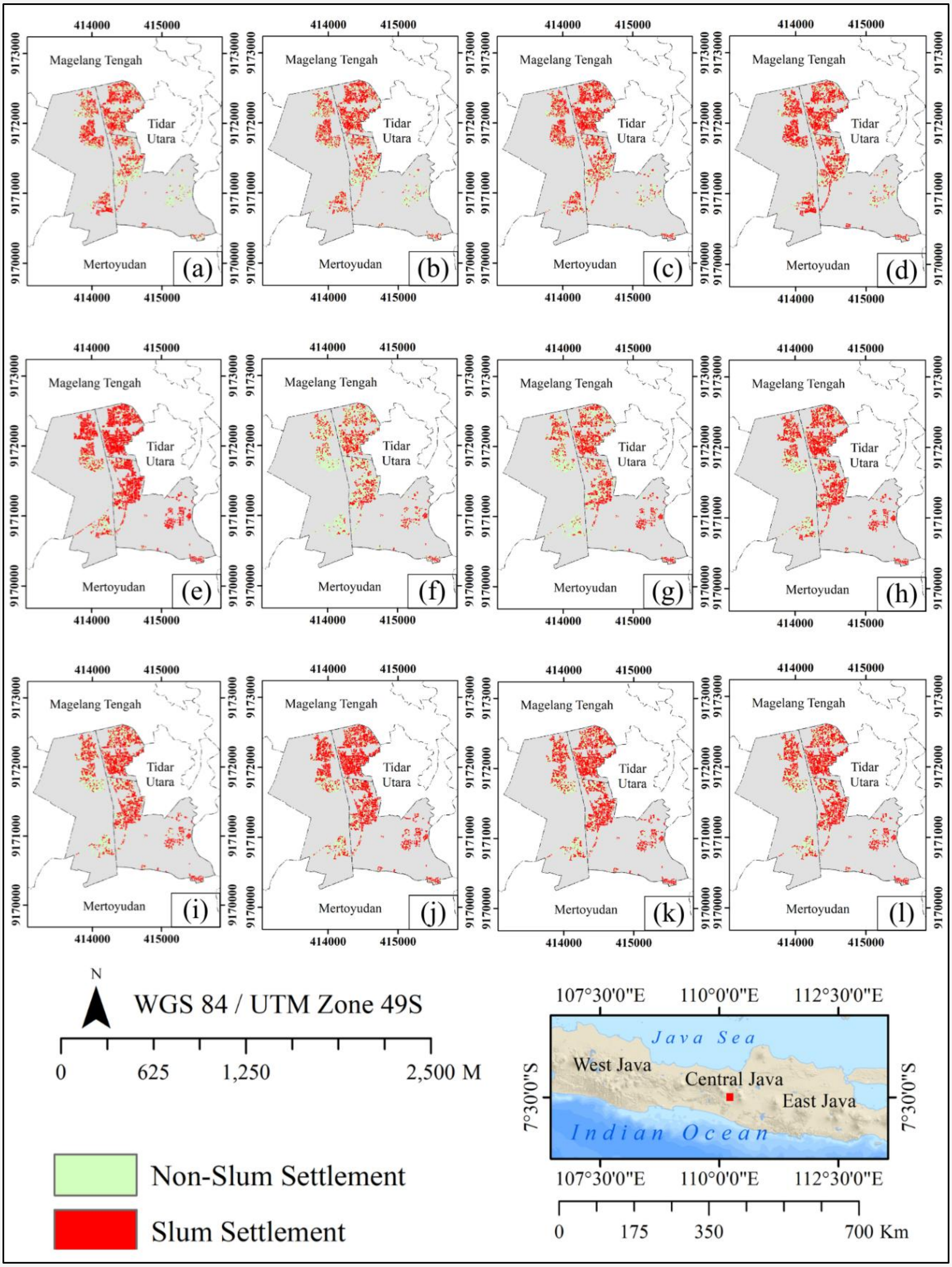


**Figure 8:** Slum and non-slum settlement classification using GLCM features: (a) Mean linear kernel (b) Mean polynomial kernel (c) Mean RBF kernel (d) Mean sigmoid kernel (e) Variance linear kernel (f) Variance polynomial kernel (g) Variance RBF kernel (h) Variance sigmoid kernel (i) Dissimilarity linear kernel (j) Dissimilarity polynomial kernel (k) Dissimilarity RBF kernel (l) Dissimilarity sigmoid kernel


ISSN: 1686-6576 (Printed) | ISSN 2673-0014 (Online) | 

This pattern was observed across all three GLCM features, particularly for the Variance and Dissimilarity features, where the classified pixels remained highly fragmented. Thus, the map appeared to have higher spatial fragmentation and offered a less realistic representation of real settlement pattern. The result confirmed the lower value of accuracy, precision, recall, and F1-score achieved in the evaluation stage.

Overall, the classification maps presented in Figure 8 indicate that the RBF kernel outperformed the other kernels in classifying slum settlement indications based on GLCM texture features. The produced map displays better cluster structure, higher class separability, and fewer spatial fragmentation effects as compared to those obtained through application of the Linear, Polynomial, and Sigmoid kernels. However, even with producing the most visually convincing result of classification, the RBF kernel achieved overall accuracy level of 62.26%. This means that uncertainty in classification is relatively high. Hence, the map generated is to be treated as a preliminary estimate of possible slum settlement distribution rather than definitive visualization of reality on the ground. In future researches, the classification results might be improved through inclusion of more features and reference data.

*3.4 Area Distribution and Spatial Patterns*

The estimate values of slum and non-slum settlements regarding their size in the 56.27 ha study area greatly vary according to the choice of kernel as shown in Table 5. In this case, the Linear kernel resulted in the highest value of the slum settlement area (31.49 ha) because it smoothes the boundary between the classes, that is, regions which possess features resembling slums are classified as slum settlements. This was linked to the complexity of settlement conditions in the Magersari, South Tidar and South Rejowinangun neighbourhoods, which are characterised by high building density, narrow spacing between buildings, irregular building layouts, and variations in roofing materials and conditions. These conditions resulted in high variations in tone and texture within the satellite imagery, meaning that non-slum areas may exhibit visual characteristics resembling those of slum areas. Conversely, the Sigmoid kernel produced the most conservative estimate (24.55 ha), which could potentially lead to an underestimation of transitional areas. The RBF kernel produced a more balanced distribution, with 30.44 ha of non-slum areas and 25.83 ha of slum areas, whilst the Polynomial kernel yielded 29.28 ha of non-slum areas and 26.99 ha of slum areas. These differences indicated that the choice of kernel directly influences the results of spatial interpretation in slum mapping, as also shown in the bar chart as shown in Figure 9. From the final output of the classification result using majority voting within polygons, the spatial pattern of slums and non-slum regions appeared to be more coherent and structurally sound at the level of building object as presented in Figure 10. Slum regions were mainly located in high density regions, especially near the PT KAI railway line in Tidar and Rejowinangun Selatan.

**Table 5:** Area distribution of slum and non-slum areas across SVM kernel function

| Kernel | Non-Slum Area (ha) | Slum Area (ha) | Total Area (ha) |
|---|---|---|---|
| Linear | 24.78 | 31.49 | 56.27 |
| RBF | 30.44 | 25.83 | 56.27 |
| Polynomial | 29.28 | 26.99 | 56.27 |
| Sigmoid | 31.72 | 24.55 | 56.27 |

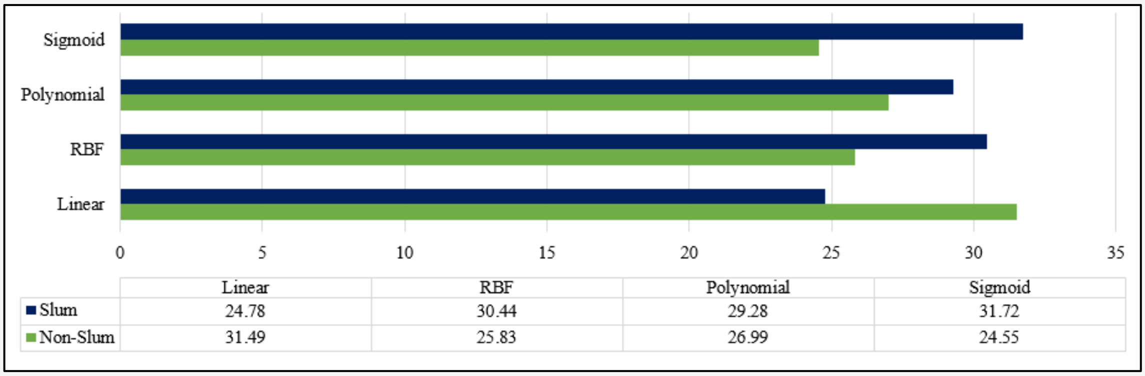


**Figure 9:** Comparison of slum and non-slum area scross SVM kernel function

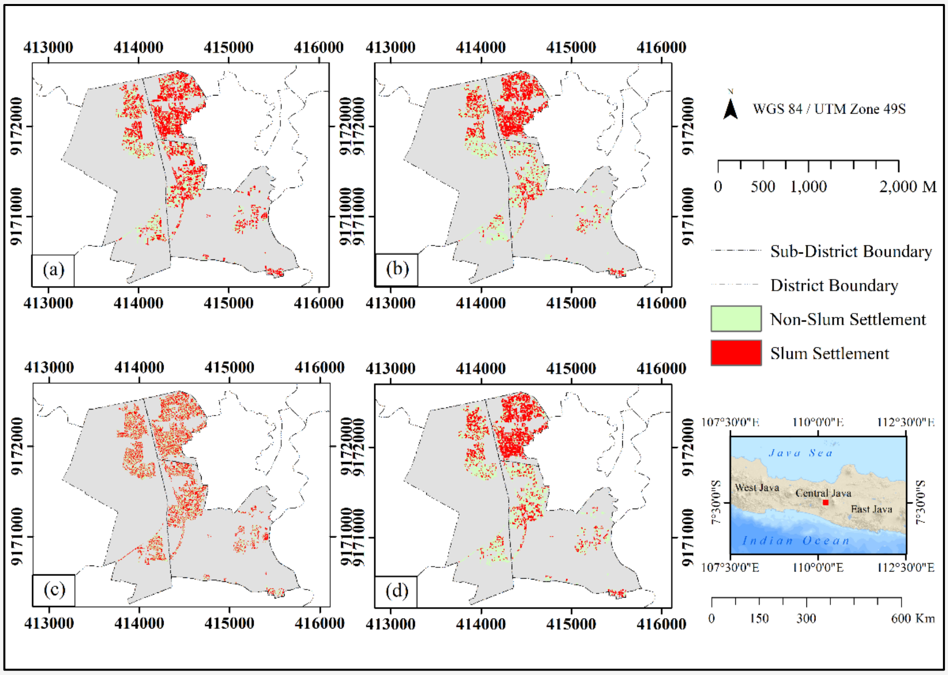


**Figure 10:** Slum and non-slum settlement classification: (a) Linear, (b) RBF, (c) Sigmoid, and (d) Polynomial

Majority voting helped in overcoming the pixel level fragmentation in classification by combining the results within polygons, giving rise to a more reliable spatial pattern that can be used in urban scale analysis. Though the end product looks to be more cohesive, the disparities among kernel functions are observed in the combined output, showing that each model is capable of doing differently while drawing boundaries for decision in the initial phase of classifying pixels. RBF kernel yields the most cohesive output, as there is cohesion of slum zones into compact clusters matching the settlement block structure in terms of morphology. The Polynomial kernel has somewhat coherent output but some level of fragmentation remains even in this case.

However, in the case of the Linear kernel, there is an appearance of more scattered distribution that is greatly dependent on road networks due to the presence of the linear nature of its decision boundary. In the Sigmoid kernel, the spatial distribution pattern is found to be the least stable as several slum patches have been found to be inconsistent or do not remain the same even after applying majority voting, meaning low flexibility to the underlying feature distribution. Hence, from the majority voting outcomes, it can be stated that though pixel-wise classification varies for all kernels, object-wise aggregation enhances spatial meaningfulness. This clearly underlined the need for spatial generalization after classification while extracting slums from GLCM texture features.

*3.5 Discussion and Implications*

The overall accuracy of 62.26% attained by the RBF model highlighted one of the key difficulties involved in urban remote sensing, which is that GLCM-based texture feature extraction alone is unable to capture all dimensions of socio-physical aspects of informal settlements [10]. This average performance demonstrated a classification limit that has been experienced by all pixel-based approaches using regular RGB images, due to the high fine scale heterogeneity resulting in severe class overlap [4] and [8]. In addition, there were quite a few False Positive misclassifications observed from the confusion matrix, which means that some non-slum pixels have been mistakenly recognized as slum pixels. This implied that the texture features derived from aerial imagery may not be able to classify formal dense settlements from informal settlements in complex urban environments. The key issues in classification arise in two different types of urban areas: dense formal residential areas characterized by compact layout producing high texture variance like slums (leading to commission error) and low-quality organized housing having regular geometric alignment despite poor construction (leading to omission error) [31]. This resulted in conflicting texture pattern, making it difficult for statistical measures to distinguish between the two. Moreover, the limitation of using RGB images restricts the capacity of classification model to capture any other environmental or structural feature that could serve as an indicator of slum. In order to tackle these shortcomings and enhance mapping accuracy, a more integrated feature space should be adopted in future research. The use of more texture features as well as multiple feature extraction algorithms can result in a better understanding of characteristics of settlement areas. Utilization of ancillary vector cadastral layers such as building footprint compactness, perimeter-to-area ratio, building density, and orientation entropy can effectively distinguish between organic and planned spatial configurations of settlements [32]. Incorporation of spectral indices such as NDVI and NDBI can effectively account for vegetation deficiency and built-up intensity typical of slums [33], while multi-temporal Synthetic Aperture Radar (SAR) coherence data can monitor the rate of structural consolidation in informal settlements [34]. Also, the use of imagery with higher number of spectral bands as well as incorporation of different source of information, including LiDAR and cadastral data, can help in identifying informal areas.

Improvements can also be found within the process of classification itself. Inasmuch as this study has concentrated on Support Vector Machine (SVM) only, future studies need to look at other machine learning and deep learning models that can perform well when applied to urban slum mapping. This would give valuable insight as to what makes certain classification methods more useful than others in relation to this kind of application. Nevertheless, such approaches generally require substantially larger training datasets and higher computational resources than the SVM-GLCM framework adopted in this study. Another critical issue is the choice of GLCM window size. For the present investigation, the window sizes were mainly selected depending on the size of the rooftops of buildings. Future studies need to use a more integrated strategy by taking into account several other factors related to space such as the size of the settlement block, layout of buildings, and density of houses. These criteria may produce more accurate texture features for the classification of slums. Finally, the consistency of time for capturing images and field survey needs to be carefully considered to avoid problems due to change in the conditions of the settlements.

Nevertheless, despite the drawbacks, this systematic assessment of the SVM-GLCM pipeline has yielded concrete empirical findings regarding urban texture analysis through scales. The transformation from pixel-based surface to building-based polygons makes up a link between machine learning results and their administrative use [34]. As applied to municipal management of Magelang City, this object-oriented approach gives an objective point of departure for local informal settlement detection. Due to the fact that the procedure employs standardized protocols for remote sensing analysis, it is capable of periodical updating with the arrival of new high-resolution imagery data for data-driven monitoring of the city upgrading through such programs as KOTAKU. Thus, the introduced framework showed its capacity for the integration of remote sensing and machine learning for preliminary and fast cost-efficient detection of slum settlements.

## 4. Conclusion

The present work explored the efficacy of applying GLCM-based texture features along with the SVM classification technique for the detection of the presence of slum settlements using high resolution aerial imagery. It was observed that both texture feature and SVM kernel selection have played a significant role in the classification process. Out of all the kernels tested, RBF kernel performed best with an accuracy of 62.26%. It was the most effective kernel for slum settlements classification as per the present study. It was also been found out that different texture features require different window sizes to define the settlement properties. It was observed that the Mean and Dissimilarity texture features have shown the best discriminatory power between the slum and non-slum classes, showing the significance of choosing proper texture features and scales in the analysis of urban textures. The obtained classifications helped in defining the spatial distribution patterns of slum settlement indicators within the area under study. Despite the moderate level of accuracy, the constructed models were capable of offering an overall image of the spatial distribution of both slum and non-slum settlements. The use of the majority voting technique also helped in increasing the reliability of the obtained classifications. Thus, this study proved the effectiveness of the combination of GLCM textures and SVM classification as a potentially useful tool for slum settlement mapping. The obtained classification results can be considered as additional input data for the monitoring and planning tasks related to urban areas, and can become a basis for further research with the addition of various other features and datasets and the application of more complex classification techniques to improve the accuracy of slum settlement mapping.

**Acknowledgements**

The authors would like to express sincere appreciation and thanks to the Department of Public Works and Spatial Planning (DPUPR) of Magelang City and the Magelang City Government for their cooperation especially in giving access to all data and information needed in conducting this research.

The authors would also like to thank the Master Program of Remote Sensing, Faculty of Geography, Gadjah Mada University for giving their academic support and research facilities in completing this research.

**References**

[1] United Nations Human Settlements Programme (UN Habitat). (2003). *The Challenge of Slums: Global Report on Human Settlements 2003*. London; Sterling, VA: Earthscan Publications Ltd.

[2] Nugraha, A. T. and Zuharnen, Z., (2015). Analisis Faktor Faktor yang Mempengaruhi Perkembangan Permukiman Kumuh di Kota Magelang.[ Analysis of Factors Influencing the Development of Slums in Magelang City] *Jurnal Pembangunan Wilayah dan Kota,* Vol. 11(2); 145–158.

[3] Danarko, A. I. and Prakoso, B. S. E., (2018). Potensi Permukiman Padat sebagai Dasar Perencanaan Pembangunan Hunian Vertikal di Kota Magelang [The Potential of Dense Settlements as a Basis for Planning Vertical Housing Development in Magelang City]. *Jurnal Bumi Indonesia,* Vol. 7(3).

[4] Kuffer, M., Pfeffer, K. and Sliuzas, R., (2016). Slums from Space: 15 Years of Slum Mapping using Remote Sensing. *Remote Sensing,* Vol. 8(6). https://doi.org/10.3390/rs8060455.

[5] Kohli, D., Sliuzas, R., Kerle, N. and Stein, A., (2012). An Ontology of Slums for Image Based Classification. *Computers, Environment and Urban Systems,* Vol. 36(2); 154–163.

[6] Mattos, A. B., (2021). Mapping Slums with Medium Resolution Satellite Imagery. *Remote Sensing Applications: Society and Environment,* Vol. 24. https://doi.org/10.1016/j.rsase.2021.100642.

[7] Haralick, R. M., Shanmugam, K. and Dinstein, I. H., (1973). Textural Features for Image Classification. *IEEE Transactions on Systems, Man, and Cybernetics*, Vol. 3(6); 610–621.

[8] Kuffer, M., (2020). The WorldPoverty Map: Mapping Informal Settlements with Deep Learning and Satellite Imagery. *Remote Sensing,* Vol.12(14). https://doi.org/10.3390/rs12142245.

[9] Georganos, S., (2021). Scale and Processing Effects in Deep Learning Based Slum Mapping. *International Journal of Applied Earth Observation and Geoinformation,* Vol. 102. https://doi.org/10.1016/j.jag.2021.102400.

[10] Persello, C. and Stein, A., (2017). Deep Fully Convolutional Networks for the Detection of Informal Settlements. *IEEE Geoscience and Remote Sensing Letters,* Vol. 14(12); 2325–2329. https://doi.org/10.1109/LGRS.2017.2763738.

[11] Mountrakis, G., Im, J. and Ogole, C., (2011). Support Vector Machines in Remote Sensing: A Review. *ISPRS Journal of Photogrammetry and Remote Sensing,* Vol. 66(3); 247–259. https://doi.org/10.1016/j.isprsjprs.2010.11.001.

[12] Schölkopf, B. and Smola, A. J., (2002). *Learning with Kernels.* Cambridge, MA: MIT Press.

[13] Balqis, H., Hidayati, I., and Susilo, B. (2026). Comparison of Built-Up Expansion Prediction Models for Magelang City and Its Peri Urban Areas: CA-Logistic Regression, CA-SVM, CA-MLP, and CA-RF. *International Journal of Geoinformatics*, Vol. 22(5), 89–112. https://doi.org/10.52939/ijg.v22i5.4982.

[14] Wijaya, F., Saputra, R. and Alamsyah, D., (2016). Implementasi Metode Interpolasi Bicubic Modifikasi. [Implementation of Modified Bicubic Interpolation Method] *JATISI,* Vol. 2(2); 87–94. https://doi.org/10.35957/jatisi.v2i2.48.

[15] Congalton, R. G. and Green, K., (2019). *Assessing the Accuracy of Remotely Sensed Data: Principles and Practices (3rd ed.).* Boca Raton, FL: CRC Press.

[16] Géron, A., (2019). *Hands on Machine Learning with Scikit Learn, Keras, and TensorFlow (2nd ed.).* Sebastopol, CA: O'Reilly Media.

[17] Alwi, B., (2020). *Analisis Kesesuaian Lahan Permukiman pada Kawasan Bandung Utara Menggunakan Sistem Informasi Geografi*. [Analysis of Land Suitability for Residential Development in the North Bandung Area Using Geographic Information Systems], Universitas Gadjah Mada.

[18] Christiawan, P. I., (2019). Tipe Urban Sprawl dan Eksistensi Pertanian di Wilayah Pinggiran Kota Denpasar. [Urban Sprawl Types and Agricultural Existence in the Outskirts of Denpasar City]. *Jurnal Wilayah dan Lingkungan,* Vol. 7(2); 79–89. https://doi.org/10.14710/jwl.7.2.79-89.

[19] Haralick, R. M., (1979). Statistical and Structural Approaches to Texture. *Proceedings of the IEEE,* Vol. 67(5); 786–804.

[20] Duque, J. C., Patino, J. E. and Betancourt, A., (2017). Exploring the Potential of Machine Learning for Automatic Slum Identification from VHR Imagery. *Remote Sensing,* Vol. 9(6). https://doi.org/10.3390/rs9060455.

[21] Plaza, A., (2009). Recent Advances in Hyperspectral Image Processing. *Remote Sensing of Environment,* Vol. 113; S110–S122. https://doi.org/10.1016/j.rse.2008.10.011.

[22] Fadhilah, A., (2021). *Identifikasi Awal Parameter Permukiman Kumuh Berbasis Informasi Spektral dan Tekstur pada Citra Resolusi Spasial Menengah*. [Initial Identification of Slum Settlement Parameters Based on Spectral and Textural Information in Medium Spatial Resolution Images]. Universitas Gadjah Mada.

[23] Fo Boonma, R., Suwanprasit, C., Homhuan, S., and Shahnawaz, (2024). Classification of Northern Thai Rice Varieties Using Random Forest (RF) and Support Vector Machine (SVM) on Google Earth Engine with Sentinel Imagery: A Case Study in Buak Khang Subdistrict, San Kamphaeng District, Chiang Mai Province. *International Journal of Geoinformatics*, Vol. 20(9), 27–42. https://doi.org/10.52939/ijg.v20i9.3539.

[24] Refaeilzadeh, P., Tang, L. and Liu, H., (2009*). Cross Validation.* Encyclopedia of Database Systems. Springer. New York.

[25] Cohen, J., (1960). A Coefficient of Agreement for Nominal Scales. *Educational and Psychological Measurement,* Vol. 20(1); 37–46. https://doi.org/10.1177/001316446002000104.

[26] Fathilda, I. K., (2023). *Analisis Data Penginderaan Jauh dalam Mengenali Indikator Permukiman Kumuh di Kota Semarang.* [Remote Sensing Data Analysis in Identifying Slum Settlement Indicators in Semarang City], Universitas Gadjah Mada. [Online]. Available: https://etd.repository.ugm.ac.id/penelitian/detail/232676. [Accessed: Jul. 4, 2026].

[27] United Nations Human Settlements Programme (UN Habitat). (2016). *Slum Almanac 2015–2016: Tracking Improvement in the Lives of Slum Dwellers. Nairobi: UN Habitat.* [Online]. Available: https://unhabitat.org/slum-almanac-2015-2016. [Accessed: Jul. 4, 2026].

[28] Burges, C. J. C., (1998). A Tutorial on Support Vector Machines for Pattern Recognition. *Data Mining and Knowledge Discovery*, Vol. 2(2); 121–167. https://doi.org/10.1023/A:1009715923555.

[29] Hsu, C. W., Chang, C. C. and Lin, C. J., (2003). *A Practical Guide to Support Vector Classification.* Taipei: Department of Computer Science, National Taiwan University. [Online]. Available: http://www.csie.ntu.edu.tw/~cjlin/papers/guide/guide.pdf. [Accessed: Jul. 4, 2026].

[30] Chang, C., C. and Lin, C., J., (2011). LIBSVM: A Library for Support Vector Machines. *ACM Transactions on Intelligent Systems and Technology,* Vol. 2(3); 1–27. https://doi.org/10.1145/1961189.1961199. [Accessed: Jul. 4, 2026].

[31] Hofmann, P., Strobl, J., Blaschke, T. and Kux, H., (2008). *Detecting Informal Settlements from QuickBird Data in Rio de Janeiro Using an Object Based Approach.* In T. Blaschke, S. Lang, & G. J. Hay (Eds.), Object Based Image Analysis (pp. 531–553). Berlin; Heidelberg: Springer.

[32] Wurm, M. and Taubenböck, H., (2018). Detecting Social Groups from Space. *Remote Sensing Letters,* Vol. 9(1); 41–50. https://doi.org/10.1080/2150704X.2017.1411234. [Accessed: Jul. 4, 2026].

[33] Bhatta, B., (2018). *Remote Sensing and GIS (3rd ed.).* Oxford University Press. New Delhi.

[34] Blaschke, T., Hay, G. J., Kelly, M., Lang, S., Hofmann, P., Addink, E., Queiroz Feitosa, R., van der Meer, F., van der Werff. H., van Coillie, F. and Tiede, D., (2014). Geographic Object Based Image Analysis – Towards a New Paradigm. *ISPRS Journal of Photogrammetry and Remote Sensing,* Vol. 87; 180–191. https://doi.org/10.1016/j.isprsjprs.2013.10.014.